Design and Optimization of Piezoresistive MEMS Pressure Sensors Using ABAQUS

Nabiollah Abol Fathi and Zohreh Allah Moradi

Amirkabir University of Technology

Abstract: In this paper, optimization of a piezoresistive Micro Electro Mechanical System (MEMS) pressure sensor has been intended. The aim of this study is to find an optimal diaphragm shape by Finite Element Method (FEM) using ABAQUS®, which is the most suitable software in this area. Optimal diaphragm shape is a one, that results in reasonable output stimuli with maximal deflection and minimal stress. Three different shapes of diaphragms are considered in this study, they are circular, square and rectangular diaphragms. Another purpose of this study is to find out the effect of holes in these diaphragms. With respect to applied stress and sensor output, results were showing that circulate shaped diaphragms are performing much more efficient than other shapes. Rectangular holes have better influence on the function of diaphragms too.

Key words: MEMS piezoresistive pressure sensor · Wheatstone bridge · Diaphragm shape · Holes

INTRODUCTION

Pressure sensors are widely used in automotive, medical and various types of industrial applications [1, 2]. MEMS devices have very low power consumption; besides they require very low space.

In this work, it is assumed that Wheatstone bridge configuration is used to sense the stress developed in a diaphragm. The stress is sensed by measuring change in piezoresistors which are connected in Wheatstone bridge configuration that are situated on a pressure sensor diaphragm. The pressure is converted into a electrical signal by the use of resistance change phenomena due to the stress or strain of the piezoresistors. The stress or strain causes electrical signal fluctuations in two ways, one way is by structural deformation induced resistance variations and the other way is by the quantum physical phenomena induced resistivity variations.

Three different shapes of diaphragms have been compared together. Stress, deflection, sensor output voltage and sensitivity of Circular, square and rectangular shapes of diaphragms have been examined.

The diaphragm shapes that have been simulated in FEM software are shown in Fig. 1. The dimensions of the diaphragm are such that the area is same in all the three cases.

Sensor Diaphragm Design: In order to model the silicon pressure sensor diaphragm, it is assumed that the diaphragm has a uniform thickness, with perfectly clamped edges. In the steady state, the diaphragm deflection is governed by the Lagrange equation as in eqn. (1) which allows to calculate the out-of-plane membrane deflection $w(x,y)$ as a function of position [3-4]. In this case, Cartesian coordinates are chosen for analysis as the diaphragm is rectangular in shape.

$$\frac{\partial^4 w(x,y)}{\partial x^4} + 2\alpha_{si} \frac{\partial^4 w(x,y)}{\partial x^2 \partial y^2} + \frac{\partial^4 w(x,y)}{\partial y^4} = \frac{P}{Dh^3}$$
(1)

P represents the differential pressure applied on the membrane of thickness h; D is a rigidity parameter which depends on material properties given by eqn. (2)

$$D = \frac{E h^3}{12(1-v^2)}$$
(2)

The anisotropy coefficient α_{si} depends on the crystallographic orientation. E is the Young's modulus whereas v is the Poisson's ratio. The factor G is called the shear modulus or Coulomb Modulus and it describes the reaction of the material to the shear stress. α_{si} Can be calculated using eqn. (3) and eqn. (4).
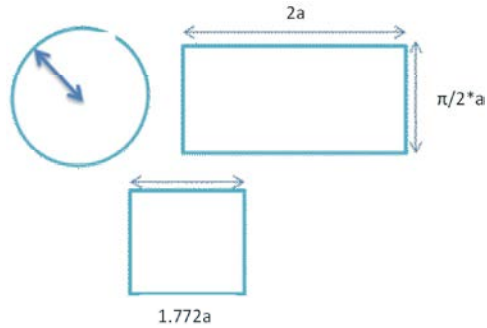
Corresponding Author: Nabiollah Abol Fathi, Amirkabir University of Technology, Iran.

Fig. 1: Circular, square and rectangular diaphragms and their relative dimensions used in simulations

$$G = \frac{E}{2(1+\upsilon)} \tag{3}$$

$$\alpha_{si} = \upsilon + \frac{2G(1-v^2)}{E} \tag{4}$$

However the exact solution of eqn. (1) does not exist and one of the approaches used to analyze the basic shapes is the Polynomial approximation [5-6]. This approach is used to analyze the deflection and stress for the different shapes of diaphragms.

Circular Diaphragm: Considering the isotropic circular membrane of radius *a* as shown in Fig. 1, which is characterized by the axial symmetry. So in order to simplify calculations, the out of plane deformation *w(r)* is considered to be dependent only on the distance from its center *r* and is given by eqn. (5) [7].

$$w(r) = \frac{Pa^4}{64D} \left[1 - \frac{r^2}{a^2}\right]^2 \tag{5}$$

Square Diaphragm: The solution to eqn.(1) for a square diagram with side length of $\sqrt{\pi\alpha}$ as shown in Fig. 1(a) is $w(x, y)$, with appropriate approximations and simplification yields the displacement of a square diaphragm which changes with uniform pressure (P), given by eqn. (5) [7].

The solution to eqn. (1) for a square diaphragm with side length of 2a as shown in Fig. 1 is *w(x,y)* with appropriate approximations and simplification yields the displacement of a square diaphragm which changes with uniform pressure (P), given by eqn. (6) [7].

$$\omega(x, y) = \frac{1}{47} \frac{Pa^4}{D} \left[\frac{1-x^2}{\pi a^2}\right]^2 \left[\frac{1-y^2}{\pi a^2}\right]^2 \tag{6}$$

Rectangular Diaphragm: In case of a rectangular diaphragm, the deflection in the diaphragm can be simplified as in eqn. (7) [7]. The width of rectangular diaphragm is $0.5\pi a$ and a length is 2a as shown in Fig. 1.

Table 1: Dimensions of various diaphragms in the design

Diaphragm type	Dimensions (μm)
Circular	250 (radius)
Square	443 (side)
Rectangular	396×500 (length × width)

$$\omega(x, y) = \frac{p(1-v^2)}{2Eh^3} \left[\frac{\frac{\pi^2 a^2}{16} - x^2}{\frac{\pi^4 a^4}{256} + a^4}\right]^2 (a^2 - y^2)^2 \tag{7}$$
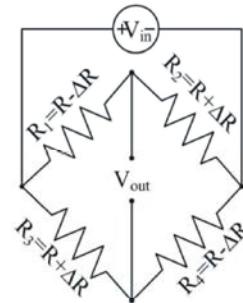

Fig. 2: Wheatstone bridge configuration to measure output voltage due to change in resistances on the sensors

Sensor Design: A pressure sensor is designed to measure a pressure from 1MPa to 100 MPa. The diaphragm thickness (h) is estimated as 30μm and made on plane of single crystalline silicon. For the rectangular diaphragm design, a length to width ratio of 1.25 is assumed. Various diaphragm dimensions are shown in Table 1. The Young's modulus (E) of Si is 2×1011 Pa and Poisson's ratio (υ) is 0.28 [8].

Sensor Circuit Design: A Wheatstone bridge circuit as shown in Fig. 2 is used for sensing the output voltage [9]. Four piezoresistors namely R1, R2, R3 and R4 form the bridge circuit.

The length, width and thickness of the piezoresistors are 200μm, 10μm and 10μm respectively. The piezoresistors are placed with an offset (distance from the edge of the diaphragm) of 13μ m in the longitudinal direction and 10μm in the transverse direction. The electrical resistivity of each piezoresistor is 0.5×10^{-4} Ωm.

When no pressure is applied, the bridge is under balance and ΔR is zero and the output voltage of the sensor is zero. When a pressure is applied, the resistance of the piezoresistors change thus the bridge is not balanced which results in a voltage at the output. As the applied pressure results in more diaphragm deflection, that causes more stress and more output voltage. Thus the bridge output voltage is a direct indication of the applied pressure.

Stress Concentration Region: Another thing that will be considered in this area is the effect of holes on the diaphragms. The main concept for this approach is to increase stress that occurred on diaphragms. SCR (Stress Concentration region) is an approach where defects or holes are made in order to increase stress. To produce SCR, no extra high tech equipment is needed; because it just involves etching and mask design. So, this approach appears to be the most suitable for enhancing the sensitivity of piezoresistive MEMS since the piezoresistive material has good sensitivity to stress and no additional complicated equipment or process are required [9-12].

In this paper the effect of three different shapes of hole have been studied in all considering diaphragms. Maximum stress, maximum deflection and maximum sensitivity in each case had been calculated [13-15].

Application Mode Using ABAQUS: In this paper, we introduce an implementation of the extended finite element method for structural mechanics analysis. Applied approach in this article enables the use of available ABAQUS capabilities (interactive FEM mesh generation, finite element libraries and so on) in order to solve the problems presented in previous sections [16-15].

RESULT AND DISCUSSION

In this section, deflection and stress and sensitivity for all the three diaphragms under consideration are compared. Stress contours of each situation are also presenting in this section.

Effect of Diaphragm's Geometry: All of the three diaphragms are simulated using ABAQUS and various results are compared. Fig. 3 shows a comparison of Stress, maximum Sensitivity and maximum deflection in various diaphragm shapes while applied pressure is constant. It can be observed from Fig. 3 that the deflection is more in circular diaphragm. As observed in Fig. 4 the rate of change of deflection is more in case of Circular diaphragm, while rate of changing of stress in rectangular shape is bigger than the two others.

As observed from the stress counters, The Stress is minimum at the center of the diaphragm and maximum at edges. Table 2 provides a comparison between the maximum deflections, Stress and sensitivity in all the three different diaphragms at an applied pressure of 10 MPa.

Fig. 4 shows a comparison of the maximum stress and deflection in various diaphragm shapes as the applied pressure is changed. It can be observed from Fig. 4 that the stress is more in rectangular shaped diaphragm.
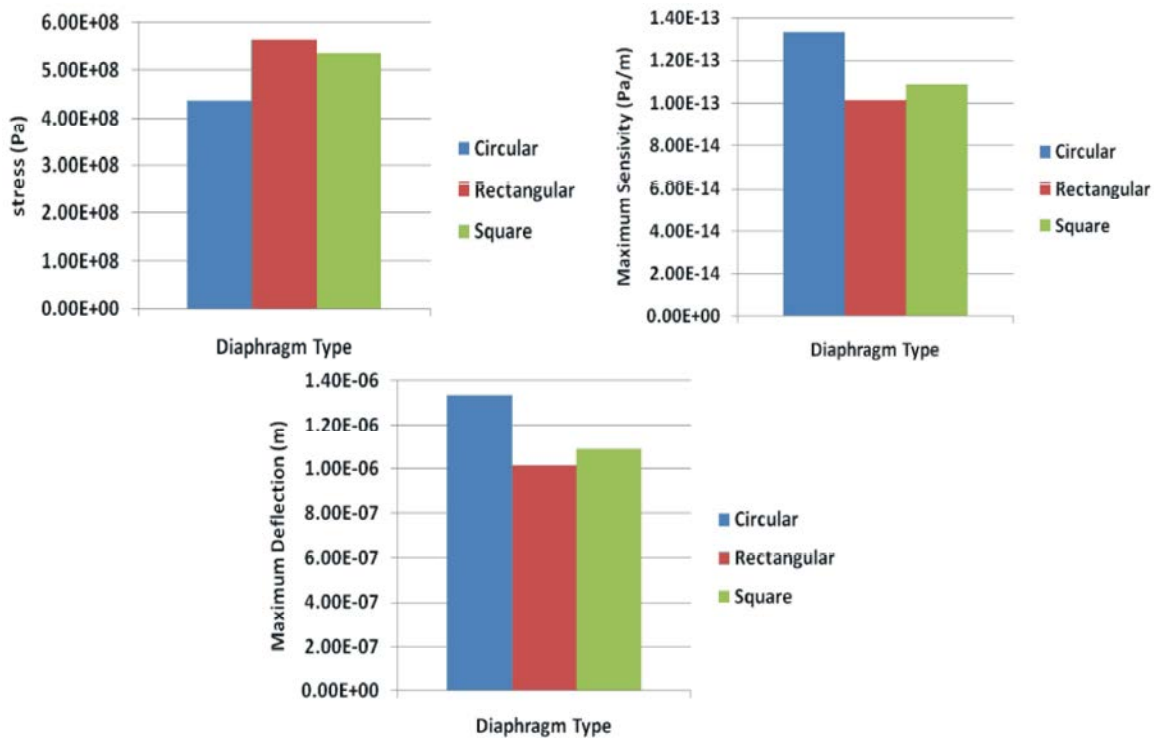

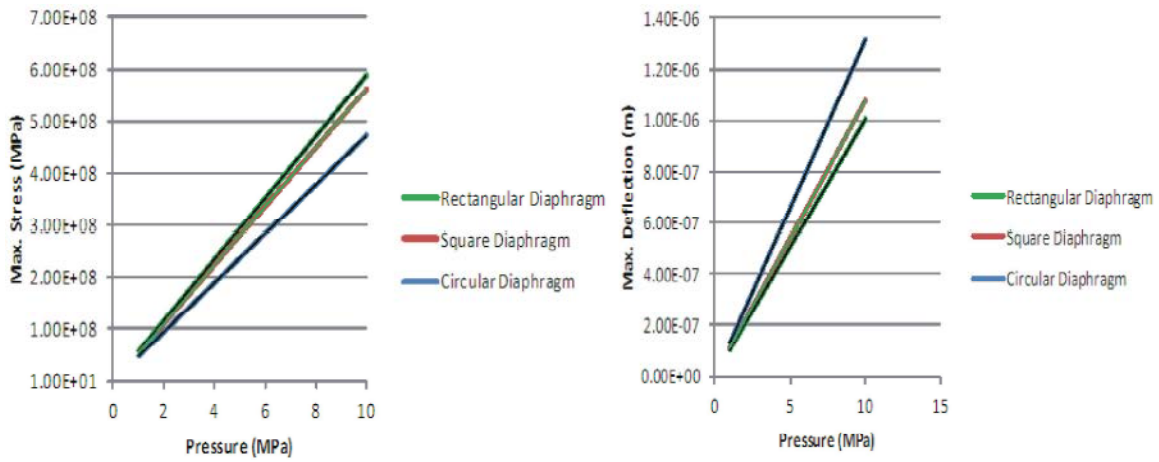Fig. 3: Stress, Maximum Sensitivity and maximum deflection in three different shapes of diaphragm

Fig. 4: Maximum Stress and maximum deflection in three different shapes of diaphragm
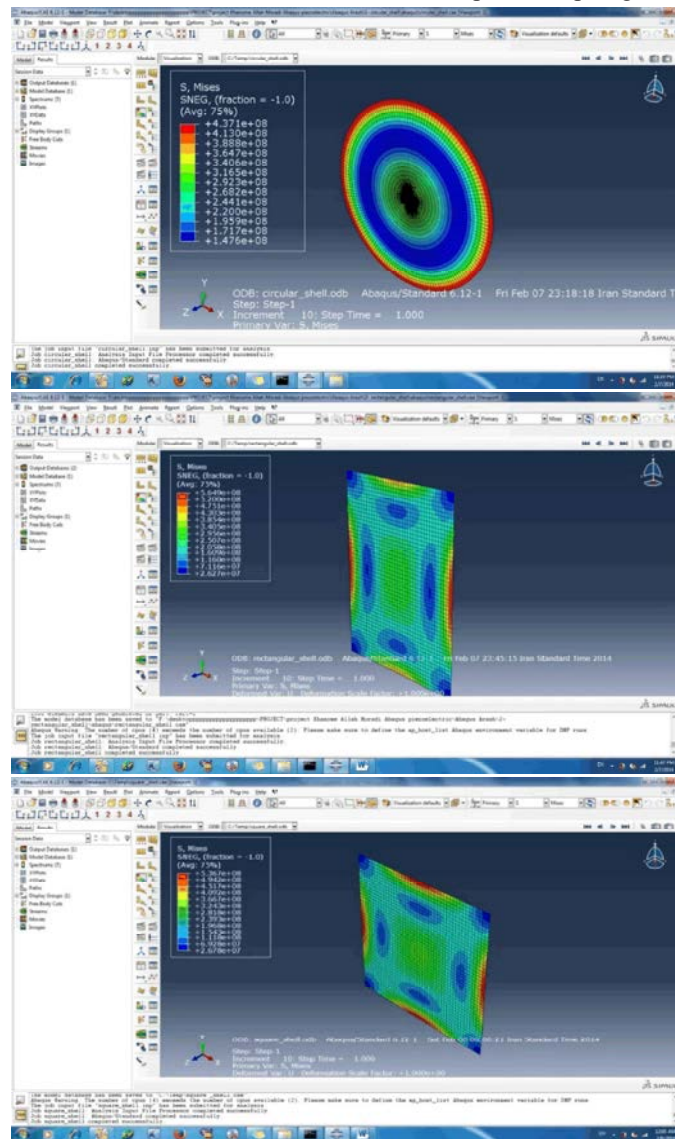

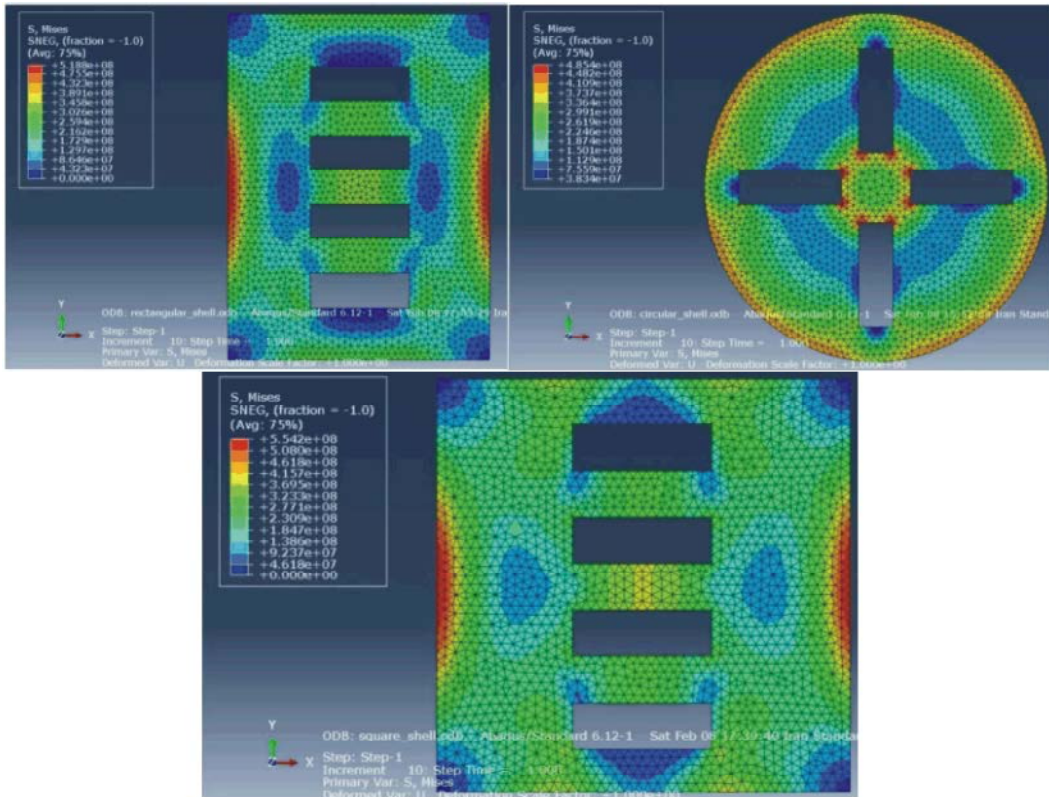Fig. 5: Stress contours in three shapes of diaphragms

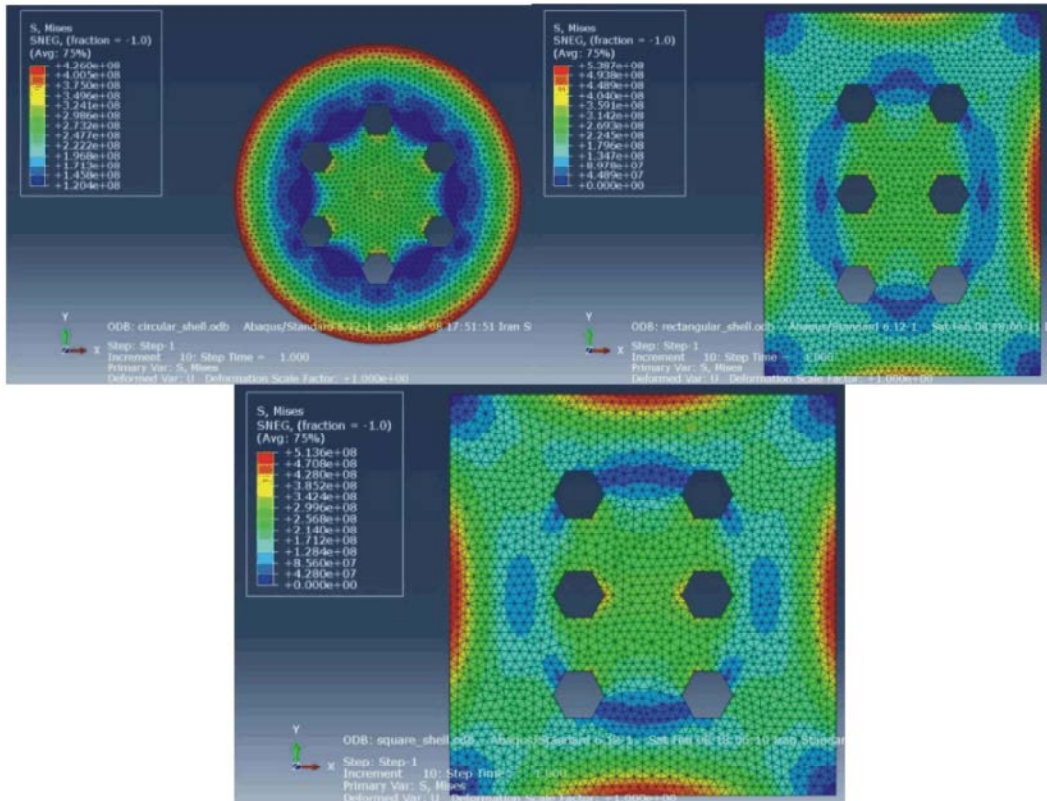Fig. 6: Stress contours in three shapes of diaphragms with rectangular holes

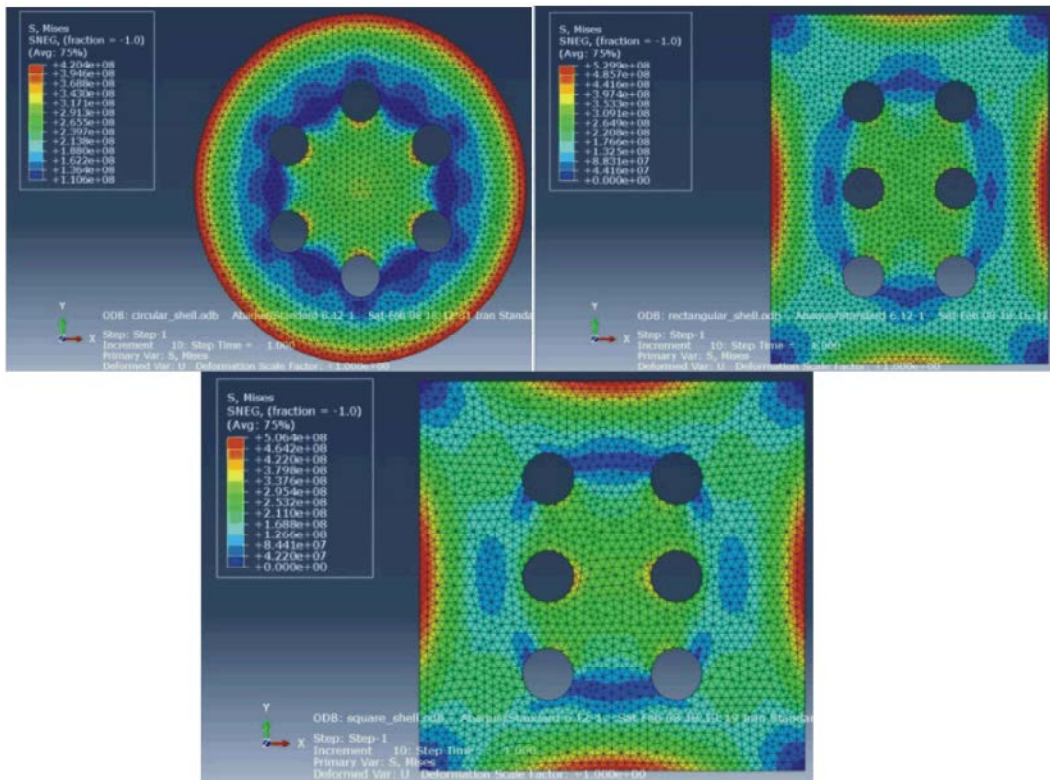Fig. 7: Stress contours in three shapes of diaphragms with hevagonal holes

Fig. 8: Stress contours in three shapes of diaphragms with circular holes

Table 2: Maximum Stress, Maximum Deflection & Maximum Sensitivity at 10 MPa applied pressure

Diaphragm Type	Applied Pressure (MPa)	Maximum Stress (Pa)	Maximum Deflection (m)	Maximum Sensitivity
Circular	10	4.37E+08	1.33E-06	1.33E-13
Rectangular	10	5.65E+08	1.01E-06	1.01E-13
Square	10	5.37E+08	1.08E-06	1.08E-13

Table 3: Maximum Stress, Maximum Deflection & Maximum Sensitivity in three shapes of diaphragms with 3 kinds of hole and without hole

Maximum Sensitivity	Maximum Stress	Maximum deflection	Hole Type	Geometry of Diaphragm
1.437e-13	4.854e8	1.437e-6	Rectangular	Circular
1.282e-13	4.260e8	1.282e-6	Hevagonal	
1.273e-13	4.204e8	1.273e-6	Circular	
1.330e-13	4.371e8	1.330e-6	without hole	
1.058e-13	5.188e8	1.058e-6	Rectangular	Rectangular
1.007e-13	5.387e8	1.007e-6	Hevagonal	
1.002e-13	5.299e8	1.002e-6	Circular	
1.013e-13	5.649e8	1.013e-6	without hole	
1.361e-13	5.542e8	1.361e-6	Rectangular	Square
1.078e-13	5.136e8	1.078e-6	Hevagonal	
1.074e-13	5.064e8	1.074e-6	Circular	
1.084e-13	5.367e8	1.084e-6	without hole	

Table 2 provides a comparison between the maximum deflections in all the three different diaphragms at an applied pressure of 10MPa. It can be noted that in a rectangular diaphragm, the stress is much larger compared to other diaphragm shapes. This is due to the fact that, the diaphragm structure is more asymmetric.

Mechanical Analysis of the Effect of Holes on Diaphragms: Table 3 summarizes the analysis result of stress, deflection and sensitivity difference for different types of SCR holes in each diaphragm type. In Fig. 6-8 stress contours in three shapes of diaphragms with different kinds of hole have been compared together.

CONCLUSION

In this research, three different shapes of diaphragm have been simulated in ABAQUS. From FEA results, circular type diaphragm had better function. This subsumption is based on the comparison between stress and deflection results in these three kinds of diaphragms. However, when the stress in the diaphragm is considered, the rectangular diaphragm feels more stress compared to the square diaphragm. Thus, the probability for the sensor breakdown is more in the rectangular diaphragm when compared to the square diaphragm. To reduce stress, one can increase the diaphragm thickness. In conclusion circular typed diaphragms are more preferred than the other two shapes, namely square and rectangular diaphragms.

From another view when we added holes in diaphragms, significant differences have been observed. The piezoresistive MEMS with circular diaphragms and rectangular holes had more sensitivity compared to other situations.

REFERENCES

1. Lin, L. and W. Yun, 1998. MEMS pressure sensors for aerospace applications, Aerospace Conference, IEEE, 1: 429-436.
2. Aravamudhan, S. and S. Bhansali, 2008. Reinforced piezoresistive pressure sensor for ocean depth measurements, Sensors and Actuators A., 142: 111-117.
3. Sathishkumar, R., A. Vimalajuliet, J.S. Pra-sath, K. Selvakumar and S.V. Reddy, 2011. Microsize ultrasonic transducer for marine applications," Indian Journal of Science and Technology, 4(1): 8-11.
4. Li, X. and M. Bao, 2001. Micromachining of multi thickness sensor-array structures with dual stage etching technology," Journal of Micro- mechanics and Micro Engineering, 11: 239-244.
5. Herrera-May, A.L., B.S. Soto-Cruz, F.L´opez-Huerta and L.A. Aguilera Cort´es, 2009. Electromechanical analysis of a piezoresistive pressure Micro Mexicana De Fi´sica, 55(1): 14-24.
6. Blasquez, G. and Y. Naciri, 1987. Static response of capacitive pressure sensor with square or rectangular silicon Diaphragm" Journal of Applied Physics, 22/7: 505-510.
7. Khakpour, R., R. Solmaz, M. Mansouri and A.R. Bahadorimehr, 2010. Analytical Comparison for Square, Rectangular and Circular Diaphragms in MEMS Applications, International Conference on Electronic Devices.
8. Kattabooman, N. and S. Sarath, 2012. VLSI Layout Based Design Optimization of a Piezoresistive MEMS Pressure Sensors Using COMSOL, COMSOL conference in Bangalore.
9. Lin, J.M., 2004. Teaching and Design on Smart MEMS Pressure Sensor Module, International Conference on Engineering Education and Research Progress through Partnership, ICEER, pp: 273-281.
10. Sh Mohd Firdaus and Husna Omar,"High Sensitive Piezoresistive Cantilever MEMS Based Sensor by Introducing Stress" Finite Element Analysis-New Trends and Developments, Chapter, 11: 225-250.
11. Bhatti, M.A., C.X. Lee, Y.Z. Lee and N.A. Ahmed, 2007. Design and Finite Element Analysis of Piezoresistive Cantilever with Stress Concentration Holes. 2nd IEEE Conference on Industrial Electronics and Applications.
12. Chollet Frank and Liu Haobing, 2007. A short introduction to MEMS. Micromachines Centre, School of MAE, Nanyang Technological University, Singapore.
13. Amar Khennane, June 10, 2013. Introduction to Finite Element Analysis Using MATLAB® and Abaqus.
14. David, V. and Hutton David Hutton, Fundamentals of Finite Element Analysis -0072922362-McGraw Hill-20.
15. Zienkiewiczand, O.C. and R.L. Taylor, 2000. The Finite Element Method: The Basis, 5th edition, Volume1, Butterworth-Heinemann, Oxford.